

RESEARCH

Open Access



Identification of RC3H1 as antiviral host factor binding to the non-structural protein 1 of Influenza A virus via a 3-stage computational pipeline and cell-based analysis

Swee Teng Teo¹, Shamima Rashid², Kong Yen Liew¹, Kah Man Lai¹, Teng Ann Ng², Jifeng Jiao³, Chee Keong Kwoh² and Yee-Joo Tan^{1*}

Abstract

To complete its life-cycle in the infected host, Influenza A virus (IAV) hijacks host machineries by expressing multiple viral proteins to bind to specific host proteins. In the era of integrative genomics, there is an opportunity to develop computational techniques to accurately and quickly predict host-pathogen protein-protein interactions (HP-PPI). Our 3-stage computational pipeline shortlisted host proteins (of which stages (i) and (ii) have been previously reported) containing the C3H zinc finger domain as putative interactors of the non-structural protein (NS1) of A/PR8/34 (H1N1), which is a well-characterized laboratory strain. To assess the accuracy of this computational pipeline, the top 7 highest scoring C3H zinc finger proteins were examined in co-immunoprecipitation experiments to determine which pair(s) of interaction is detectable in mammalian cell lines. Interestingly, one of them is CPSF30 which is a known NS1 binder. For the other 6 C3H zinc finger proteins, they have not been reported to be involved in IAV replication and co-immunoprecipitation experiments reveals that 4 of them bind to NS1. As a proof-of-concept, one shortlisted C3H protein was studied using live IAV infection and the knockdown of RC3H1 slightly increased the production of progeny virion, suggesting that it acts as an antiviral host factor.

Keywords Influenza A virus, RC3H1, NS1, C3H zinc finger protein

*Correspondence:

Yee-Joo Tan

mictyj@nus.edu.sg

¹Infectious Diseases Translational Research Programme, Department of Microbiology and Immunology, Yong Loo Lin School of Medicine, National University of Singapore, Singapore, Singapore

²School of Computer Science and Engineering, Nanyang Technological University, Singapore, Singapore

³Yingkou Institute of Technology, Yingkou City, Liaoning Province, China



© The Author(s) 2025. **Open Access** This article is licensed under a Creative Commons Attribution-NonCommercial-NoDerivatives 4.0 International License, which permits any non-commercial use, sharing, distribution and reproduction in any medium or format, as long as you give appropriate credit to the original author(s) and the source, provide a link to the Creative Commons licence, and indicate if you modified the licensed material. You do not have permission under this licence to share adapted material derived from this article or parts of it. The images or other third party material in this article are included in the article's Creative Commons licence, unless indicated otherwise in a credit line to the material. If material is not included in the article's Creative Commons licence and your intended use is not permitted by statutory regulation or exceeds the permitted use, you will need to obtain permission directly from the copyright holder. To view a copy of this licence, visit <http://creativecommons.org/licenses/by-nc-nd/4.0/>.

Introduction

Influenza, commonly known as the flu, is a highly contagious acute respiratory disease caused by influenza viruses that infect respiratory tracts through aerosol transmission or bodily fluid contact. Most influenza infections are caused by influenza A virus (IAV), which often causes seasonal epidemics or occasionally pandemics due to frequent mutations in its genome [1]. As IAVs are able to infect different avian and mammalian species, there is a high risk for humans to acquire infections through zoonotic transmission. This not only makes it difficult to eradicate the virus, but also allow for the generation of potentially pandemic strains due to the insufficient human immunity and lack of readily available therapeutics to combat the new spillover viruses [2]. IAV belongs to the family Orthomyxoviridae and is an enveloped RNA virus containing a single-stranded, negative sense, segmented RNA genome comprising of 8 segments of viral RNA (vRNA), which encode 11 known proteins [3]. The viral proteins are generally categorized into 2 groups, the structural and the non-structural proteins.

The majority of the research on IAV focuses on the structural proteins which are components present in the mature assembled virus and are further categorized into surface proteins and internal proteins. On the other hand, the non-structural proteins are viral proteins that are expressed only in the host cells but not in the virus itself. They are mostly involved in the suppression of host-immune systems, determining virulence and facilitating pathogenesis [4].

In order to understand the role of IAV proteins in mediating the virulence of infection, we previously curated dataset of lethal dose studies of IAV infection in mice [5] and used it to map IAV-mouse proteome wide domain-domain interaction [6]. Briefly, this involved the retrieval of mouse host proteins sequences because IAV virulence studies are mainly conducted in mice and subjecting them to domain assignment with SUPERFAMILY 2.0. Similarly, each viral protein of the commonly studied A/PR8/34(H1N1) (abbreviated as PR8) virus was assigned to at least one SCOP domain. Via DISPOT, the C3H zinc finger (C3H-ZF) domain in mouse proteins was predicted to be interacting significantly with the non-structural protein (NS1) of PR8 [6].

The NS1 protein is an immunomodulatory factor used by IAV to counteract host immune responses [7]. It is composed of two main functioning domains: RNA-binding domain (RBD) at the N-terminal, and the effector domain near the C-terminal that predominantly mediates interactions with host cell proteins. These two domains are connected by a linker region [8]. NS1 is a multifunctional protein that has functions in innate immunity suppression, shutting off host gene

expression, inducing apoptosis, facilitating viral replication and determining virulence [3]. NS1 has distinctive roles in both the cytoplasm and nucleus [3]. In the cytoplasm, it has the following functions. It limits induction of interferon- β (IFN- β) through binding to cytoplasmic pathogen (dsRNA) sensor, retinoic acid-inducible gene I (RIG-I) [9–13]. It also restricts the host antiviral state by blocking the function of the dsRNA activated cytoplasmic antiviral proteins 2'-5'- oligoadenylate synthetase (OAS) [14] and the dsRNA-dependent serine/threonine protein kinase R (PKR) [15]. A predominant function of NS1 RNA-binding domain is to out-compete OAS for interaction with dsRNA, thereby inhibiting this host antiviral strategy [14]. As for PKR, it has been proposed that NS1 could possibly bind to a linker region in PKR and thereby preventing a conformational change that is normally required for the release of PKR auto-inhibition [16]. NS1 enhances viral mRNA translation by interacting with eukaryotic translation initiation factor 4GI (eIF4GI), poly(A)-binding protein I (PABI) and hStaufen, to recruit viral mRNAs to multi-protein translation initiation complexes [3]. It recruits eukaryotic translation initiation factor eIF4I, the large subunit of the cap-binding complex eIF4E, to the 5'UTR of viral mRNAs, thereby increasing viral translation [17]. It also been shown to interact with poly(A)-binding protein I (PABI), a known interactor of eIFGI [18]. In addition, NS1 can interact and cause the redistribution of hStaufen, a dsRNA and tubulin protein related to PKR, which normally contributes towards microtubular transport of cellular mRNAs to sites of enhanced translation like polysomes [19]. Interaction of hStaufen with NS1 could possibly promote efficient viral mRNA translation. Furthermore, NS1 is known to regulate apoptosis by activating the PI3K/Akt pathway to delay apoptosis, providing enough time for the virus to replicate within host cells [20].

On the other hand, NS1 has the following functions in the nucleus to inhibit cellular pre-mRNA processing and shutting off host gene expression. It can target and inhibit PABII, which hinders the poly-A tail synthesis and results in accumulation of mRNA with short poly-A tail [21]. It can also bind to the Cleavage and Polyadenylation Specificity Factor 4 (CPSF30, also known as CPSF4), a key host protein that regulates the polyadenylation step of pre-mRNA processing [22]. CPSF30, which contains 5 tandem C3H-ZF repeats, is also found to be involved in the recognition of the AU-hexamer sites [23], the site upstream to the polyadenylation cleavage site that is critical for the addition of poly-A tail to the 3' end of mRNA. Previous studies reported that NS1 protein shuts off host gene expression by interacting with and blocking CPSF30, a host pre-mRNA processing protein, which led to the accumulation of host pre-mRNA [24]. It is also

reported that the effector domain of NS1 interacts with CPSF30 at its 2nd and 3rd zinc finger region [25].

Our previous computational pipeline predicts that mouse proteins with C3H zinc finger (C3H-ZF) motif interact with NS1 and there are many proteins containing this domain. In general, zinc finger (ZF) proteins contain the zinc finger domains which comprise of a combination of cysteine and histidine residues that may serve as ligands for zinc ions from other proteins. Upon binding of zinc to these ligands, the domain adopts the structure necessary for function [22]. ZF domains typically occur in tandem repeats and are often associated with DNA or RNA binding as well as binding to other proteins. ZF proteins are very abundant in cells and have a wide range of functions with their DNA or RNA binding abilities, including gene regulation, target degradation, DNA repair and antiviral responses [26]. One important class of ZF proteins is the C3H-ZF proteins, which serve as RNA-binding proteins that regulate RNA metabolism. The C3H-ZFs are characterized by one or more C3H zinc finger domains containing three cysteine residues and one histidine residue [27].

The interaction of the C3H-ZF protein known as CPSF30 with NS1 is well-established as described above. However, there are multiple C3H-ZF proteins in the human host but little is known about their roles in IAV infection and if the C3H-ZF motif within the full-length protein is accessible to bind to NS1 in the same way as CPSF30. Here, an additional refinement step was added to our previous computational pipeline so as to identify specific human C3H-ZF proteins that are most likely to bind to NS1 of PR8. The output from the improved 3-stage computational pipeline provides a list of human C3H-ZF proteins as putative NS1 binders. To assess the accuracy of this prediction, the top 7 hits in the shortlist were then subjected to co-immunoprecipitation experiments to determine if they interact with NS1 in human cell lines. As a proof-of-concept, infection study was then used to determine if one of the novel and validated NS1-host interactions can enhance or inhibit viral replication.

Materials and methods

Computational prediction of IAV-host interactions

Computational prediction of IAV and human host protein interactions was done in three stages as follows: (i) domain assignment with SUPERFAMILY 2.0 [28] using structural folds, (ii) domain-domain interaction prediction using Domain Interaction Statistical Potential (DISPOT) [29] and finally, refinement of DISPOT predictions with (iii) the human-virus PPI web server (HVPPPI) [30] that uses protein sequence embeddings with a random forest classifier. The stages of (i) and (ii) were completed in a project on IAV-mouse proteome wide domain-domain interaction study and published previously [6].

Based on this, mouse proteins containing the C3H-ZF motif are predicted to bind the NS1 of IAV. As there are multiple proteins containing the C3H-ZF motif, stage (iii) was developed here to identify specific human C3H-ZF protein(s) binding to NS1 of PR8 by using the human-virus PPI (HVPPPI) web server (<http://zzdlab.com/hvppi/predict.php>) [31] which implements an unsupervised sequence embedding approach, doc2vec to represent protein sequences as rich feature vectors of low dimensionality. Then, these vectors were used as inputs to train a random forest (RF) classifier to predict human-virus PPIs. Sequences of human C3H proteins were paired with the NS1 segment of PR8, forming the input to HVPPPI. Lastly, HVPPPI automatically calculates and outputs the interaction probability of a query protein pair. In this experiment, to identify if two proteins interact, the 0.90 specificity threshold was referenced, corresponding to a probability score of at least 0.143.

Cell lines, plasmids and virus

293FT cells were purchased from Thermo Scientific while COS-7, H1299 and MDCK cells were purchased from ATCC. They were cultured in DMEM containing 10% FBS and grown in a 37°C incubator with 5% CO₂. The NS1 ORF of PR8 was cloned into the pXJ40myc vector with a myc-tag at the 5' end. The human C3H ZF ORFs were purchased from Genscript and have flag tags at the 3' end. Influenza/A/Puerto Rico/8/1934 (PR8) was produced via reverse genetics system and titered via plaque assay as previously described [32].

Co-immunoprecipitation (co-IP) performed with transfected cells

In order to perform co-IP to verify the interaction between NS1 and human C3H ZF proteins shortlisted computationally, 293FT cells were transfected with the respective flag-tagged ZF and myc-tagged NS1 using either lipofectamine 2000 (Invitrogen) or X-tremeGENE 360 (Roche). The cells were lysed in RIPA buffer (50mM Tris-HCl (pH 8.0), 150mM NaCl, 0.5% NP-40, 0.5% sodium deoxycholate and 1mM phenylmethylsulfonyl fluoride) and the cell lysates were then incubated with flag-beads (Sigma) overnight. The beads were extensively washed with binding buffer (50mM Tris-HCl (pH 8.0), 150mM NaCl, 0.5% NP-40, 0.5% sodium deoxycholate), boiled in 1X Laemmli SDS sample buffer and separated by SDS-PAGE. After SDS-PAGE, Western blot (WB) analysis was performed. The primary antibodies used for WB are anti-myc (Santa Cruz Biotechnology), anti-flag (Millipore) and anti-NS1 [33].

Immunofluorescence

H1299 cells seeded on cover slips in 24-well plates were transfected with myc-tagged NS1 and/or flag-tagged

ZF using X-tremeGENE 360 (Roche). After 24 h, the cells were washed with PBS and fixed with 4% paraformaldehyde. After permeabilization with 0.2% Triton-X 100 in PBS and blocking with 10% FBS in PBS, the cells were then stained with mouse anti-myc antibody (Santa Cruz Biotechnology) (1:500) or rabbit anti-flag antibody (Millipore) (1:800). This was followed by the incubation with goat anti-mouse IgG (H+L) secondary antibody, Alexa Fluor™ 568 or anti-rabbit IgG (H+L) secondary antibody, Alexa Fluor™ 488 (Invitrogen) diluted 1:500 in blocking solution. The cell nuclei were stained with DAPI (Invitrogen). The immunofluorescence images under the magnification of 20X were taken using Olympus CKX53 microscope.

Subcellular fractionation

H1299 cells were either mock or infected with PR8 at MOI of 5. At 24 h post infection (hpi), cells were harvested in 1xPBS using cell scraper and subjected to subcellular fractionation using Nuclear/Cytosolic Fractionation Kit (Cell Biolabs) according to the manufacturer's protocol. Fractionated cell lysate was subjected to WB analysis to examine the cellular localization of RC3H1 and MKRN1 in mock- and PR8-infected cells. The primary antibodies used are anti-RC3H1 (Invitrogen), anti-MKRN1 (Bethyl Laboratories), anti-GAPDH (Merck) and anti-lamin A (Santa Cruz). Densitometry analysis was performed using Image Lab software (Bio-Rad) to quantify the expression of proteins in different subcellular fractions. The relative levels of RC3H1 and MKRN1 in cytosol and nuclear fractions were calculated by normalizing against total expression of proteins in both fractions.

Co-immunoprecipitation (co-IP) performed with infected cells

In order to perform Co-IP to verify the interaction between NS1 and RC3H1, H1299 cells were either mock or infected with PR8 at MOI 5. At 48 h post infection (hpi), the cells were lysed in RIPA buffer (50mM Tris-HCl (pH 8.0), 150mM NaCl, 0.5% NP-40, 0.5% sodium deoxycholate and 1mM phenylmethylsulfonyl fluoride) and cell lysates were then incubated with home-made mouse monoclonal antibody (mAb) 19H9 [34] on a rocker for 1 h at 4 °C to allow the 19H9 mAb to bind to NS1 protein in the lysates. After which, a mixture of Protein A and G beads (Roche) were added, followed by incubation at 4 °C overnight. The beads were washed with binding buffer (50mM Tris-HCl (pH 8.0), 150mM NaCl, 0.5% NP-40, 0.5% sodium deoxycholate) 4 times before being boiled in 1X Laemmli SDS sample buffer to release all bound proteins and subjected to western blot analysis to detect for co-immunoprecipitated NS1 and RC3H1 proteins. To detect the presence of NS1 protein, rabbit anti-NS1

antibody [33] was used as the primary antibody and Clean-Blot™ IP Detection Reagent (HRP) (Thermo Scientific) as secondary antibody. To detect the presence of RC3H1, rabbit anti-RC3H1 (Invitrogen) was used as the primary antibody and Goat anti-Rabbit IgG (H+L) Secondary Antibody, HRP (Invitrogen) was used as secondary antibody. To accommodate the MW of RC3H1 and NS1, different percentage of acrylamide were used for SDS-PAGE. Thus, the eluate from the Protein A/G beads was divided based on total volume into 2 portions in roughly 1:4 ratio. The bigger volume was used for detection of RC3H1.

SiRNA transfection and IAV infection

Control and RC3H1 siRNA (Invitrogen) were transfected at 40nM (80pmol per well) into H1299 cell using RNAimax (Invitrogen) for 24 h followed by reseeding into 12 well plates at 1.5×10^5 cells per well. For the siRNA transfection, 0.3ul of RNAimax for each pmol of siRNA was used. After another 24 h, the cells were infected with PR8 at MOI of 1. After 1 h of virus adsorption onto the cells, the virus-containing supernatant was completely removed and the cells in each well were washed with 1 ml of PBS. The PBS was discarded and 500 μ l of fresh medium wash added to each well and incubated at 37 °C and 5% CO₂. At 15 hpi, the cell culture supernatant was collected and subjected to plaque assay to measure progeny virion production. A separate set of reseeded cells were harvested for WB analysis to verify the knockdown efficiency. The primary antibodies used for WB are anti-RC3H1 (Invitrogen), anti-C23 (Santa Cruz Biotechnology).

Results

Identification of C3H zinc finger proteins as putative interactors of NS1 of Influenza A virus

A three-stage protocol comprising of (i) domain assignment, (ii) domain-domain interaction prediction (DDI) and (iii) refinement with a protein-protein interaction (PPI) prediction tool was used to generate a list of host proteins as putative binders of NS1 of IAV.

Stages (i) and (ii) had previously been reported in our work on IAV-mouse proteome wide domain-domain interaction study [6]. Stage (iii) represents new results that are reported here. Figure 1 shows the whole computational protocol and additional details can be found in the Supplementary file.

Based on stages (i) and (ii), the C3H-ZF domain in mouse proteins was predicted to be interacting significantly with NS1 of PR8 virus [6]. However, the function of a protein in a biological system is dependent on the secondary and tertiary structures of a protein which are dependent on its full sequence. Therefore, in this work, we added stage (iii) as a refinement to predict if the

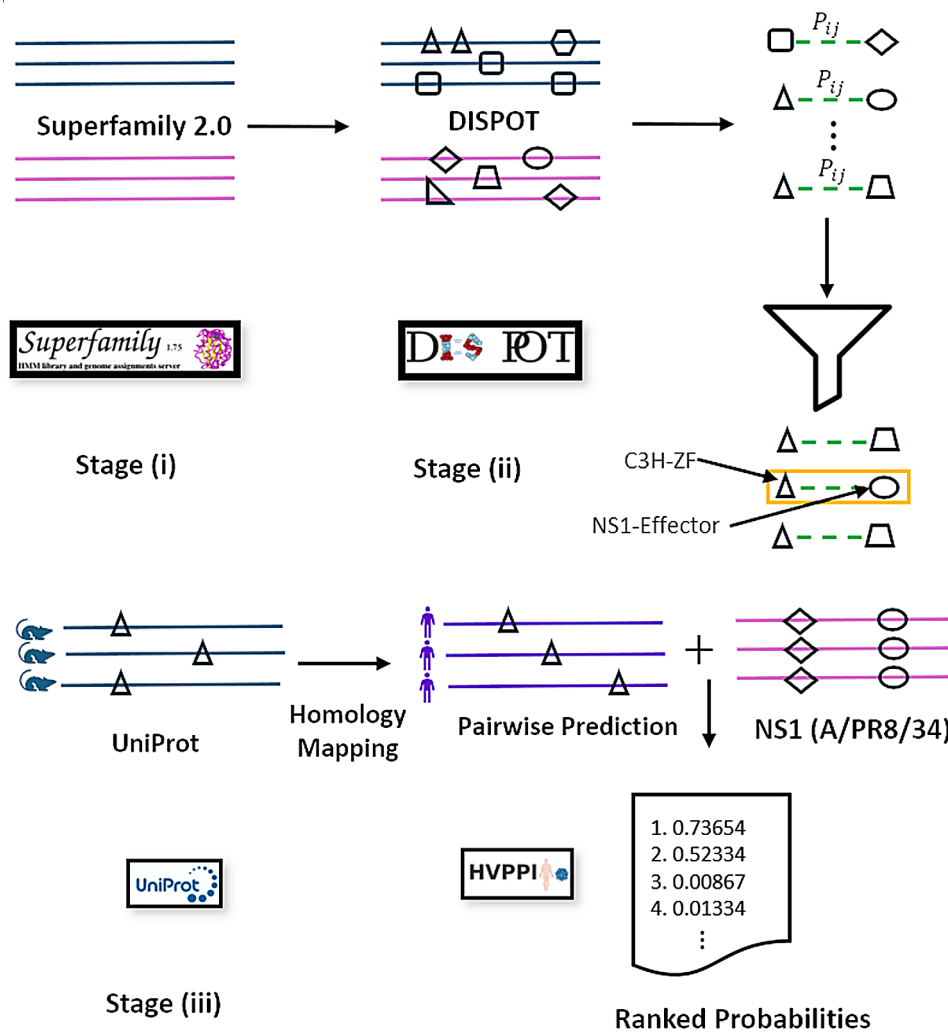


Fig. 1 Overview of the computational protocol. In stage (i), SCOP domains were assigned to mouse and viral protein sequences (shown as blue and pink lines, respectively) using SUPERFAMILY2.0. In stage (ii), DISPOT was used to identify highly likely domain-domain interactions based on probabilities (P_{ij}) derived using statistical potentials. The C3H ZF domain in mouse proteins and NS1 effector domain in IAV viral proteins was identified as a significant interaction (indicated with an orange rectangle). In stage (iii), an additional evaluation was performed to refine the candidate pairs that are likely to be interacting. First, the mouse sequences with C3H-ZF domains were converted to human sequences (shown in purple) by homologous assignment. Next pairwise interaction prediction (between human and PR8 NS1 viral sequences) was performed with the Human-Virus PPI server to obtain a ranked probability list identifying 21 likely pairs. Of these, a final 7 were shortlisted for wetbench experimental evaluation. Logos of web tools in the figure were obtained from their respective webpages

C3H-ZF domain found in different human proteins can interact with NS1 of PR8 virus based on their full-length protein sequences.

For stage (iii), the 17,120 mouse proteins were analysed and 35 of them were found to contain the C3H-ZF domain. As C3H-ZF proteins have different length and other functional motifs, HVPPI was applied to predict the ability of each of them to bind to NS1. To enable functional studies with human cell lines, the human protein sequences of C3H-ZF genes were obtained through mouse-human homology mapping using UniProt (<https://www.uniprot.org/>). Then, these 35 human proteins were paired with NS1 of PR8 virus to form the input

to HVPPI. From this, 21 human C3H-ZF proteins were identified as putative interactors of NS1 of PR8 (supplementary Table 1). To assess the accuracy of this prediction, the top 7 hits in the shortlist were then subjected to co-immunoprecipitation experiments to determine if they interact with NS1 in human cell lines (Table 1). Interestingly, one of them is CPSE30 which has been shown to bind to NS1 and modulate viral replication [24]. For the other 6 C3H-ZF proteins, they have not been reported to be involved in IAV replication.

Table 1 Top 7 HVPPI scorers of C3H-ZF proteins predicted to bind NS1 of PR8

Gene	Accession Number ¹	UniProtID (Mouse)	UniProtID (Human)	HVPPI Score ²	Number of ZF motifs ³	Protein length (amino acids)	MW (kDa)	Subcellular Localization ³	Co-IP Result ⁴
CPSF30	NM_006693.4	Q8BQZ5	O95639	0.747	5	269	30	Nucleus	Positive
ZC3H15	NM_018471	Q3TIV5	Q8WU90	0.639	2	426	49	Cytoplasm, Nucleus	Negative
PPP1R10	NM_002714.4	Q80W00	Q96QC0	0.475	1	940	99.07	Nucleus	Negative
ZC3H8	NM_032494.3	Q9JJ48	Q8N5P1	0.353	3	291	34	Nucleus	Positive
MKRN1	NM_013446.4	Q9QXP6	Q9UHC7	0.332	4	482	53.4	Cytosol	Positive
ZC3H18	NM_001294340.2	Q0P678	Q86VM9	0.307	1	953	109	Nucleus	Positive
RC3H1	NM_172071	Q4VGL6	Q5TC82	0.294	1	1133	126	Cytoplasm, P-body, Cytoplasmic granule	Positive

¹ Accession number of gene retrieved from Genbank

² Human-virus PPI probability score calculated using HVPPI web server

³ Number of ZF motifs and subcellular localization of C3H ZF proteins retrieved from Uniprot and QuickGO

⁴ NS1-C3H-ZF protein interactions as determined by co-IP in this study

Validation of NS1-C3H-ZF protein interactions by co-IP

Plasmids containing C3H-ZF genes with a flag tag at the C terminus were used to transfect 293FT cells together with myc-tagged NS1 of PR8 virus. The expression of each C3H-ZF and NS1 were verified by WB (Fig. 2) and the flag-tagged C3H-ZF proteins were immunoprecipitated by flag antibody beads. Recently, it was shown that the interaction of NS1 of PR8 with CPSF30 results in alternative polyadenylation in infected cells while other IAV strains binds CPSF30 at higher affinity to mediate both host shutoff and alternative polyadenylation [35]. In co-IP experiment, NS1 was observed to be co-immunoprecipitated by flag-CPSF30 as expected. NS1 did not bind to the flag antibody beads when there was no flag-tag protein, indicating that NS1 does not bind non-specifically to the beads. Out of the other 6 C3H-ZF tested, 4 of them also showed interaction with NS1 (Fig. 2). They are MKRN1, RC3H1, ZC3H8 and ZC3H18. Although PPP1R10 and ZC3H15 have high HVPPI score of 0.639 and 0.475 respectively, they did not bind to NS1 in this assay.

Localization of RC3H1 or MKRN1 in PR8-infected cells

According to Uniprot classification, among the four newly identified NS1-binders, RC3H1 and MKRN1 are located in cytoplasm, while ZC3H8 and ZC3H18 are located in nucleus (Table 1) which are the same as CPSF30. However, recent studies reported that RC3H1 and MKRN1 are present in both nucleus and cytoplasm [36, 37]. Consistent with these findings, RC3H1 and MKRN1 can be seen in both nucleus and cytoplasm of H1299 cells transfected with these flag-tagged proteins (Fig. 3, left panel). When co-transfection of RC3H1 or MKRN1 was performed with myc-tagged NS1, some colocalization signals can be observed in both locations

(Fig. 3, right panel). On the other hand, ZC3H8 and ZC3H18 seem to be localized in the nucleus during single- and co-transfection. Due to the distinctive role of NS1 in nucleus and cytoplasm, NS1-binding cytoplasmic C3H-ZF proteins may exert a mechanism of action that is different from CPSF30.

However, as the proteins were overexpressed, it is difficult to assess if there is any change in the localization of RC3H1 or MKRN1 in the presence of NS1. Moreover, transient transfection cannot easily capture the temporal expression of NS1 during viral infection. Thus, subcellular fractionation followed by WB analysis was further conducted to investigate the localization of NS1-RC3H1 or MKRN1 interactions in natural infection (Fig. 4A). The human lung cell line H1299 was chosen for infection study since we are focusing on host factors in human. As shown in Supplementary Figure S1, H1299 could be infected by PR8 at high MOI of 5. As compared to mock-infected cell, the relative level of cytosol RC3H1 in PR8-infected cell is significantly lower and vice versa for nuclear RC3H1. (Fig. 4B). This indicates that IAV infection led to increased nuclear translocation of RC3H1. On the other hand, there was no obvious change in the localization of MKRN1 when the cell was infected with PR8 (Fig. 4C). Based on fractionation experiment, the change in RC3H1 localization is small. As immunofluorescence assay showed that only ~30 to 50% of H1299 were infected (Supplementary Figure S1), this may have resulted in lower sensitivity in fractionation experiment to detect relocalized RC3H1. To overcome, this, an alternative is to study the localization of RC3H1 in mock versus infected cells via immunofluorescence staining. However, the rabbit anti-RC3H1 polyclonal antibody used in this study was found to bind to other cellular

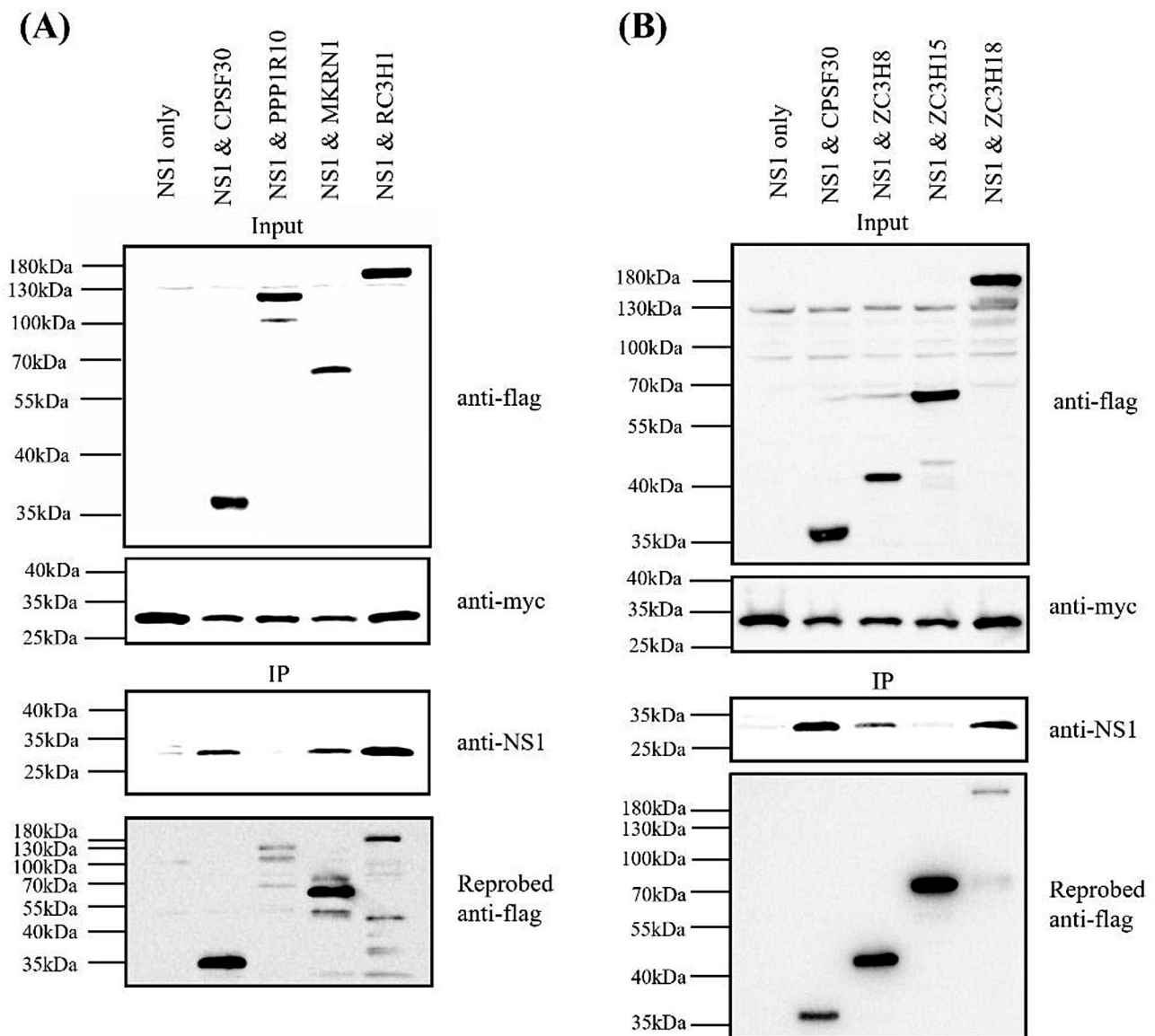


Fig. 2 293FT cells were transfected with myc-tag NS1 only or co-transfected with respective flag-tagged zinc-finger proteins. Cells transfected with myc-NS1 and flag-CPSF30 served as the positive control while cells transfected with myc-tag NS1 only served as the negative control. For **(A)**, the C3H-ZF proteins expressed are CPSF30 (MW 30 kD), PPP1R10 (MW 99 kD), MKRN1 (MW 53 kD) and RC3H1 (MW 126 kD) respectively. For **(B)**, the C3H-ZF proteins expressed are CPSF30 (MW 30 kD), ZC3H8 (MW 34 kD), ZC3H15 (MW 49 kD) and ZC3H18 (MW 109 kD) respectively. Lysates obtained from the transfected cells were subjected to WB to detect the expression levels of NS1 or flag-tagged zinc-finger proteins (top and middle panels). Flag-tagged proteins were immunoprecipitated using flag antibody beads and the levels of NS1 after IP were detected using anti-NS1 antibody (bottom panel). The levels of flag-tagged protein on the antibody beads were determined by reprobing the IP blot with anti-flag antibody. This is a representative of 3 independent experiments

proteins and it is not suitable for fluorescent microscopy (Supplementary Figure S2 and S3).

Interaction of RC3H1 with NS1 in infected cells and the impact of RC3H1 silencing on progeny virion production

The interaction between RC3H1 and NS1 in PR8-infected H1299 cells was also examined by using co-IP experiment. As shown in Fig. 5A, NS1 expressed in lysates of infected cells bound to Protein A/G beads with

NS1 monoclonal antibody. Endogenous RC3H1 was co-immunoprecipitated as it bound to NS1. In contrast, endogenous RC3H1 was not co-immunoprecipitated when lysates of mock infected cells were used with Protein A/G beads and NS1 monoclonal antibody.

Given that RC3H1 bound to NS1 in co-IP and showed increased translocation to the nucleus in IAV infected cells, the role of RC3H1 in viral replication was next examined by using RC3H1 siRNA. It has been reported

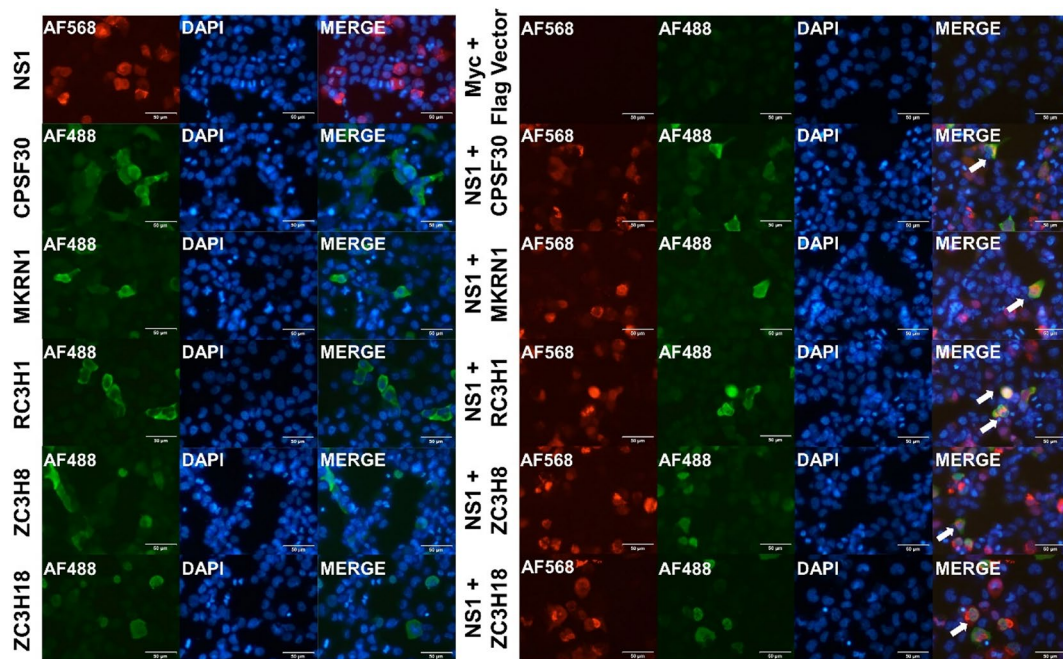


Fig. 3 H1299 cells were transfected with myc-tagged NS1, flag-tagged zinc-finger proteins or co-transfected with both plasmids. Cells transfected with myc and flag vectors served as the negative control. At 24 h post-transfection, the cells were stained with mouse anti-myc or rabbit anti-flag antibodies, followed by AF568 anti-mouse IgG (H+L) or AF488 anti-rabbit IgG (H+L) secondary antibodies. DAPI was used for nuclei staining. Magnification = 20X. Scale bar = 50 μ m. White arrows indicate co-localization signals of NS1 and zinc-finger proteins

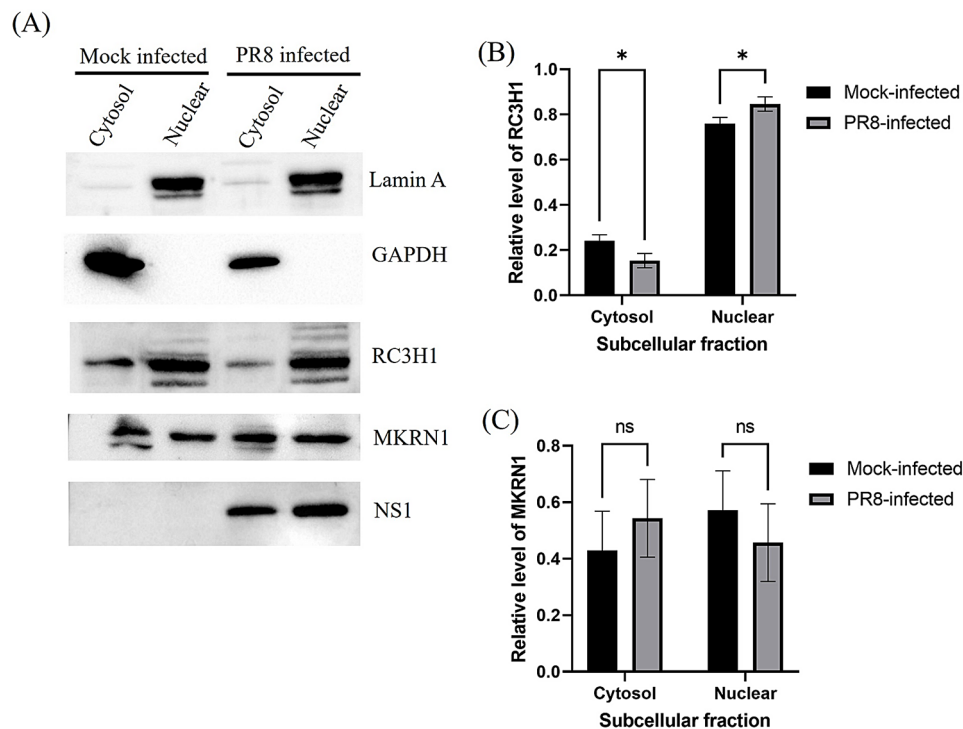


Fig. 4 H1299 cells were either mock or infected with PR8 at MOI of 5. At 24 hpi, the cells were harvested and subjected to subcellular fractionation. Fractionated cell lysate was subjected to WB analysis. **(A)** WB analysis showing the expression of NS1, RC3H1 and MKRN1 in cytosol and nuclear fractions in mock- or PR8-infected cell. GAPDH and Lamin A were used as markers for cytosol and nuclear fractions respectively. Densitometry analysis was performed to quantify protein expression. The relative levels of **(B)** RC3H1 and **(C)** MKRN1 in different subcellular fractions were plotted after normalization against total expression in both fractions. Data represented average of relative level \pm s.d. of three independent experiments and p value was calculated using two-way ANOVA followed by Šidák's multiple comparisons test. (* $p < 0.05$)

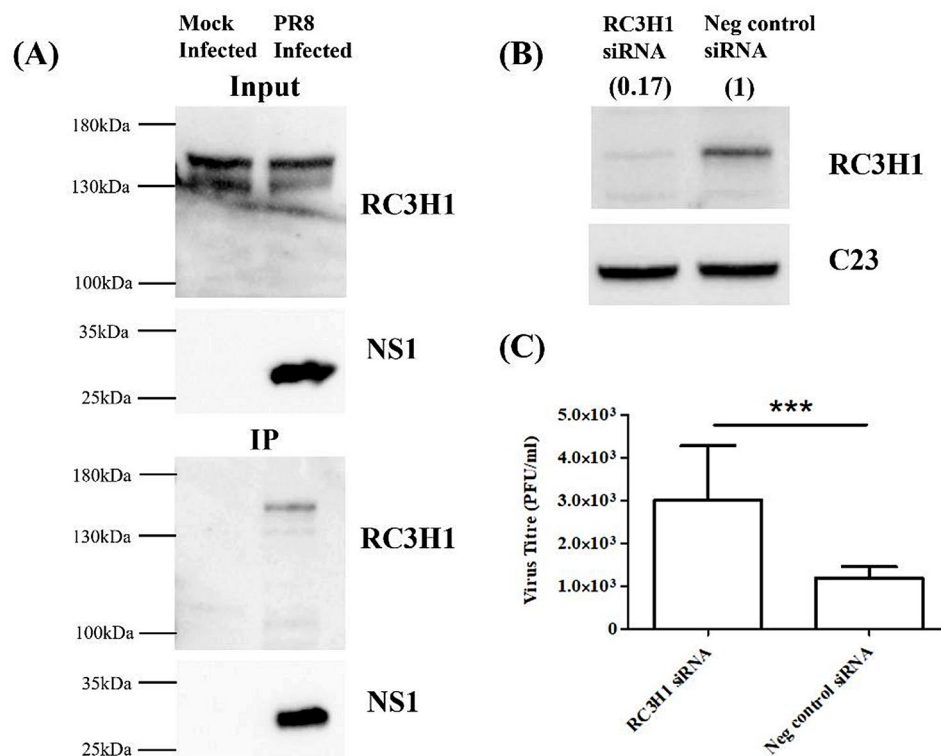


Fig. 5 (A) Co-immunoprecipitation of RC3H1 with NS1 in PR8-infected or mock-infected cells. H1299 cells were either mock or infected with PR8 at MOI of 5 and harvested at 48hpi. Lysates obtained from infected cells were subjected to WB to detect the expression levels of NS1 or RC3H1. Cell lysates were also immunoprecipitated using Protein A/G beads with NS1 monoclonal antibody and the bound proteins were eluted for WB analysis. To resolve the RC3H1 (MW ~ 126 kDa) and NS1 (MW ~ 26 kDa) proteins on SDS-PAGE, different percentages of acrylamide were used and the eluate from the Protein A and G beads was divided based into 2 portions (1:4 ratio) for detecting of NS1 and RC3H1 respectively. (B) and (C) H1299 cells were transfected with 40nM of siRNA for ~24 h followed by reseeding into 12-well plates. After another ~24 h, the cells were then infected with PR8 virus at MOI of 1. At 15 hpi, the cell culture supernatant was then collected for plaque assay on MDCK cells. A separate set of reseeded cells were harvested for WB analysis to verify the knockdown efficiency. (B) WB analysis showing the expression of RC3H1 in RC3H1 siRNA-treated and negative control siRNA-treated H1299 cells. (C) The amounts of virus produced by RC3H1 siRNA-treated and negative control siRNA-treated H1299 were compared. The average viral titer from 3 independent experiments was plotted and *p* value was calculated using Student's *t* test (***) $p \leq 0.001$

that the delivery of siRNA via lipofectamine 2000 or through siRNA-polyplexes into H1299 was more efficient in H1299 than another commonly used human lung cell line A549 [38]. Thus, we selected H1299 for RC3H1 silencing. As shown in Fig. 5B, the level of endogenous RC3H1 protein was significantly reduced upon transfection with RC3H1 siRNA when compared to control siRNA. To determine if RC3H1 silencing affects viral replication, the cells were infected with PR8 virus at MOI of 1 and harvested at 15hpi. The amount of progeny virion produced by the cells was quantified by plaque assay. Our results show that virus titer for the RC3H1 siRNA-transfected cells was significantly higher than control siRNA-transfected cells, suggesting that the knockdown of RC3H1 enhanced viral replication (Fig. 5C).

Discussion

Our computational-based approach provides a quick method to predict putative viral-host interactions. After a 3-stage sequential algorithm, a list of 21 host-encoded

C3H-ZF was predicted to be binders of NS1 of PR8 (Supplementary Table 1). To assess the accuracy of this prediction, the top 7 of them were tested for binding to NS1 protein by using co-IP binding assay performed using a human cell line. 5 out of the 7 top scorers (71.4%) bound to NS1, indicating that this pipeline produces a high level of true positive results. However, two of the predicted C3H-ZF (PPP1R10 and ZC3H15) did not bind to NS1 in the co-IP experiments despite having high HVPPI score of 0.639 and 0.475 respectively. While it is possible that another binding assay suitable for detecting their interaction with NS1 may yield a different result, it is also probable that they are false positive from our computational pipeline. Also, protein interaction predictors are often prone to false positives [39, 40]. To improve the accuracy, additional computation algorithm such as docking may be added in the future. Docking algorithms use scoring functions to evaluate predictions and could provide insight by considering 3-dimensional interactions at the interface of protein complexes. For example, recent

studies presented protocols that can yield fairly accurate prediction of protein-protein interactions using AlphaFold2-related artificial intelligence (AI) systems [41–43]. However, the accuracies of these algorithms require further assessment (e.g. only 51% of interacting pairs were able to be correctly detected using the predicted DockQ score [39]). Only 11% success rate was seen in docking of antibody-antigen complexes [41]). Hence, further investigation and development of appropriate protocols are required to determine if applying these docking protocols to the shortlisted of 21 human C3H-ZF proteins can accurately reveal which of them are true binders of NS1 of PR8.

One of the NS1-binding C3H-ZFs confirmed by the co-IP experiments is CPSF30, which is a well-characterized interactor of NS1. The interaction between NS1 of PR8 and CPSF30 does not lead to host gene shut-off but causes alternative polyadenylation in the infected cells [35]. The other 4 C3H-ZFs, namely MKRN1, RC3H1, ZC3H8 and ZC3H18, have not been documented to interact with viral proteins of IAV. According to the UniProt classification, MKRN1 and RC3H1 are found in the cytoplasm while ZC3H8 and ZC3H18 are localized in the nucleus (Table 1). In the infected cells, NS1 has distinctive roles in the cytoplasm and nucleus [3]. As CPSF30 is known to interact with NS1 in the nucleus, ZC3H8 and ZC3H18 may act on IAV in a similar way as CPSF30. As the mechanism of action for RC3H1 and MKRN1 could be different from CPSF30, subcellular fractionation was conducted to determine if the localization of RC3H1 or MKRN1 changes during IAV infection. Consistent with recent publications, MKRN1 and RC3H1 are found in both the cytoplasm and nucleus. Interestingly, there is a significant increase in the nuclear translocation of RC3H1 but not MKRN1 in IAV-infected cells. As NS1 is found in both nucleus and cytoplasm, RC3H1 may colocalize with NS1 in either compartment and modulate its function.

RC3H1, also known as Roquin-1, belongs to the Roquin family, which is one of the RNA-binding proteins (RBPs) families. In addition to the C3H1 zinc finger domain, RC3H1 has a RING finger domain and an ROQ domain at its N-terminus. The C3H1 zinc finger and ROQ domains enable RC3H1 to bind to the 3'-UTR region of target mRNAs, destabilizing them, thereby preventing excessive immune cell activation [44]. Mutations in the RC3H1 gene can result in sustained immunological inflammation due to over-activation of T follicular helper cell and the formation of germinal centers [45]. While the role of RC3H1 in maintaining immune homeostasis is well-studied, its function during viral infection remains unclear. A study by Song et al. [46] has demonstrated that RC3H1 is required for human cytomegalovirus (HCMV) lytic production. HCMV induces RC3H1 expression and

exploits it to suppress innate immune responses in primary human foreskin fibroblasts (HFFs). Mechanistically, RC3H1 binds directly to the mRNA of IRF3, blocking IRF3-mediated antiviral gene expression. As a result, the knockdown of RC3H1 increases the production of pro-inflammatory cytokines and inhibits HCMV infection [46]. These findings imply that RC3H1 has a proviral role during HCMV infection. In contrast, IAV infection does not up-regulate total RC3H1 expression in H1299 cells (data not shown). Our results show that the knockdown of RC3H1 increased the secretion of infectious PR8 virus from infected cells, indicating that RC3H1 acts as an antiviral host factor. This difference could be due to the replication mechanism of IAV being distinctive from HCMV which is a DNA virus.

NS1 protein is a key component of influenza virus that counteracts the host cell's interferon (IFN) response, thereby enhancing viral virulence [7]. As RC3H1 binds to the effector domain of NS1, it is possible that RC3H1 interferes with NS1's ability to antagonize the IFN response. Consequently, the knockdown of RC3H1 frees up more NS1 protein, enhancing viral replication through the suppression of host innate immune responses. However, the increase in viral titer in the RC3H1 knockdown cells is only 3 folds higher than the control siRNA-treated cells. This modest increase might be attributed to weak binding of RC3H1 to NS1. Alternatively, it could result from a compensatory inhibitory mechanism involving RC3H2, which is a paralog of RC3H1. RC3H1 and RC3H2 share a high degree of sequence similarity in their N-terminus and exhibit redundant functions in T cells [47, 48]. Based on our computational pipeline, RC3H2 is also predicted to bind NS1 (Supplementary Table 1). Thus, in RC3H1 knockdown cells, where the RC3H1-NS1 interaction is disrupted, RC3H2 may bind to more NS1, exerting an antiviral effect on IAV replication. This suggests that simultaneous knockdown of both RC3H1 and RC3H2 could lead to a greater increase in progeny virus production in infected cells. However, performing a double knockdown may pose challenges due to potential cytotoxicity. Further wetbench investigation will be needed to investigate whether RC3H1 interacts with the NS1 protein of different IAV strains and whether its antiviral activity is conserved across strains.

Conclusions

In summary, we have used a 3-stage computational pipeline to predict host-pathogen protein-protein interactions (HP-PPI) because this can be performed quicker and cheaper than wetbench screening methods. When applied to the PR8 IAV, the pipeline identified 21 human C3H-ZF proteins as putative interactor of NS1 and the accuracy of this prediction was assessed by subjecting the top 7 highest scoring C3H-ZF proteins to cell-based

co-IP experiment to determine which pair(s) of interaction is detectable in mammalian cell lines. We found that 5 out of the 7 top scorers (71.4%) bound to NS1, indicating that this pipeline produces a high level of true positive results but there are also false positives. As a proof-of-concept, infection study was performed on one of the novel and validated NS1-host interactions and the host RC3H1 protein was found to regulate PR8 IAV replication negatively in the human lung H1299 cell line although its influence on NS1 function appears to be low when compared to other published major mediator of NS1 function. Nevertheless, our study illustrates the development of a computational pipeline that can serve as a rapid initial screen to shortlist putative virus-binding host factors which can then be subjected to further evaluation using wetbench experiments. The limitations identified in this cross-disciplinary project will also guide future research to develop better computational pipeline for predicting virus-host interaction.

Supplementary Information

The online version contains supplementary material available at <https://doi.org/10.1186/s12985-025-02746-2>.

Supplementary Material 1

Author contributions

Y.-J.T.: Conceptualization, Writing- Reviewing and Editing. S.W.T.: Visualization, Methodology, Investigation, Writing- Original draft preparation. S.R.: Visualization, Software, Validation, Writing- Original draft preparation. K.Y.L.: Methodology, Investigation, Writing- Reviewing and Editing. K.M.L. and J.J.: Methodology, Investigation. T.A.N.: Software, Validation. C.K.K.: Conceptualization, Writing- Reviewing and Editing. All authors reviewed the manuscript.

Funding

This work is funded by Tier 2 funding (MOE2019-T2-2-175) provided by the Ministry of Education (MOE) of Singapore. JJ was funded by the Chinese Scholarship Council (CSC) to be a visiting scientist at the National University of Singapore.

Data availability

The data presented in this study are available within the article or supplementary material. No new datasets were created. However, the computational findings here are derived from bioinformatics analyses conducted in two of our previously published manuscripts. Their related weblinks are <https://iav-ppi.onrender.com/home> and <https://github.com/tengann/IAV-Host-PPI-Database/tree/main/Cleaned%20Data>.

Declarations

Ethics approval and consent to participate

Not applicable.

Consent for publication

All authors have read and agreed to this submitted version of our manuscript.

Competing interests

The authors declare no competing interests.

Received: 15 January 2025 / Accepted: 17 April 2025

Published online: 26 April 2025

References

- Rosario-Ferreira N et al. The central role of Non-Structural protein 1 (NS1) in influenza biology and infection. *Int J Mol Sci.* 2020;21(4).
- Mostafa A et al. Zoonotic potential of influenza A viruses: A comprehensive overview. *Viruses.* 2018;10(9).
- Hale BG, et al. The multifunctional NS1 protein of influenza A viruses. *J Gen Virol.* 2008;89(Pt 10):2359–76.
- Hao W, Wang L, Li S. Roles of the Non-Structural proteins of influenza A virus. *Pathogens.* 2020;9(10).
- Ivan FX, Kwok CK. Rule-based meta-analysis reveals the major role of PB2 in influencing influenza A virus virulence in mice. *BMC Genomics.* 2019;20(Suppl 9):973.
- Ng TA, Rashid S, Kwok CK. Virulence network of interacting domains of influenza a and mouse proteins. *Front Bioinform.* 2023;3:1123993.
- Ji ZX, Wang XQ, Liu XF. NS1: A Key Protein in the Game Between Influenza A Virus and Host in Innate Immunity. *Front Cell Infect Microbiol.* 2021;11:670177.
- Evseev D, Magor KE. Molecular evolution of the influenza A virus Non-structural protein 1 in interspecies transmission and adaptation. *Front Microbiol.* 2021;12:693204.
- Jureka AS, et al. The influenza NS1 protein modulates RIG-I activation via a strain-specific direct interaction with the second CARD of RIG-I. *J Biol Chem.* 2020;295(4):1153–64.
- Guo Z, et al. NS1 protein of influenza A virus inhibits the function of intracytoplasmic pathogen sensor, RIG-I. *Am J Respir Cell Mol Biol.* 2007;36(3):263–9.
- Mibayashi M, et al. Inhibition of retinoic acid-inducible gene I-mediated induction of beta interferon by the NS1 protein of influenza A virus. *J Virol.* 2007;81(2):514–24.
- Opitz B, et al. IFNbeta induction by influenza A virus is mediated by RIG-I which is regulated by the viral NS1 protein. *Cell Microbiol.* 2007;9(4):930–8.
- Pichlmair A, et al. RIG-I-mediated antiviral responses to single-stranded RNA bearing 5'-phosphates. *Science.* 2006;314(5801):997–1001.
- Min JY, Krug RM. The primary function of RNA binding by the influenza A virus NS1 protein in infected cells: inhibiting the 2'-5' oligo (A) synthetase/rnase L pathway. *Proc Natl Acad Sci U S A.* 2006;103(18):7100–5.
- Min JY, et al. A site on the influenza A virus NS1 protein mediates both inhibition of PKR activation and Temporal regulation of viral RNA synthesis. *Virology.* 2007;363(1):236–43.
- Li S, et al. Binding of the influenza A virus NS1 protein to PKR mediates the inhibition of its activation by either PACT or double-stranded RNA. *Virology.* 2006;349(1):13–21.
- Aragon T, et al. Eukaryotic translation initiation factor 4G1 is a cellular target for NS1 protein, a translational activator of influenza virus. *Mol Cell Biol.* 2000;20(17):6259–68.
- Burgui I, et al. PABP1 and eIF4G1 associate with influenza virus NS1 protein in viral mRNA translation initiation complexes. *J Gen Virol.* 2003;84(Pt 12):3263–74.
- Falcon AM, et al. Interaction of influenza virus NS1 protein and the human homologue of Staufen in vivo and in vitro. *Nucleic Acids Res.* 1999;27(11):2241–7.
- Ehrhardt C, et al. Bivalent role of the phosphatidylinositol-3-kinase (PI3K) during influenza virus infection and host cell defence. *Cell Microbiol.* 2006;8(8):1336–48.
- Chen Z, Li Y, Krug RM. Influenza A virus NS1 protein targets poly(A)-binding protein II of the cellular 3'-end processing machinery. *EMBO J.* 1999;18(8):2273–83.
- Shimberg GD, et al. Cleavage and polyadenylation specificity factor 30: an RNA-binding zinc-finger protein with an unexpected 2Fe-2S cluster. *Proc Natl Acad Sci U S A.* 2016;113(17):4700–5.
- Chan SL, et al. CPSF30 and Wdr33 directly bind to AAUAAA in mammalian mRNA 3' processing. *Genes Dev.* 2014;28(21):2370–80.
- Nemeroff ME, et al. Influenza virus NS1 protein interacts with the cellular 30 kDa subunit of CPSF and inhibits 3' end formation of cellular pre-mRNAs. *Mol Cell.* 1998;1(7):991–1000.
- Das K, et al. Structural basis for suppression of a host antiviral response by influenza A virus. *Proc Natl Acad Sci U S A.* 2008;105(35):13093–8.
- Fu M, Blakeshear PJ. RNA-binding proteins in immune regulation: a focus on CCCH zinc finger proteins. *Nat Rev Immunol.* 2017;17(2):130–43.
- Hajikhezri Z et al. Role of CCCH-Type zinc finger proteins in human adenovirus infections. *Viruses.* 2020;12(11).
- Pandurangan AP, et al. The SUPERFAMILY 2.0 database: a significant proteome update and a new webserver. *Nucleic Acids Res.* 2019;47(D1):D490–4.

29. Narykov O, Bogatov D, Korkin D. DISPOT: a simple knowledge-based protein domain interaction statistical potential. *Bioinformatics*. 2019;35(24):5374–8.
30. Yang X, et al. Prediction of human-virus protein-protein interactions through a sequence embedding-based machine learning method. *Comput Struct Biotechnol J*. 2020;18:153–61.
31. *human-virus PPI prediction: doc2vec + RF*. 2021 [cited 2023 18 October]; Available from: <http://zzdlab.com/hvppi/predict.php>
32. Wu J, et al. Biochemical and structural characterization of the interface mediating interaction between the influenza A virus non-structural protein-1 and a monoclonal antibody. *Sci Rep*. 2016;6:33382.
33. Tan Z, et al. A new panel of NS1 antibodies for easy detection and Titration of influenza A virus. *J Med Virol*. 2010;82(3):467–75.
34. Teo SHC et al. A NS1-binding monoclonal antibody interacts with two residues that are highly conserved in seasonal as well as newly emerged influenza A virus. *Pathog Dis*. 2019;77(1).
35. Bergant V, et al. mRNA 3'UTR lengthening by alternative polyadenylation attenuates inflammatory responses and correlates with virulence of influenza A virus. *Nat Commun*. 2023;14(1):4906.
36. Athanasopoulos V, et al. The ROQUIN family of proteins localizes to stress granules via the ROQ domain and binds target mRNAs. *FEBS J*. 2010;277(9):2109–27.
37. Miroci H, et al. Makorin ring zinc finger protein 1 (MKRN1), a novel poly(A)-binding protein-interacting protein, stimulates translation in nerve cells. *J Biol Chem*. 2012;287(2):1322–34.
38. Capel V, et al. Insight into the relationship between the cell culture model, cell trafficking and siRNA Silencing efficiency. *Biochem Biophys Res Commun*. 2016;477(2):260–5.
39. Tang T et al. Machine learning on protein-protein interaction prediction: models, challenges and trends. *Brief Bioinform*. 2023;24(2).
40. Sunny S, et al. DeepBindPPI: Protein-Protein binding site prediction using attention based graph convolutional network. *Protein J*. 2023;42(4):276–87.
41. Bryant P, Pozzati G, Elofsson A. Improved prediction of protein-protein interactions using AlphaFold2. *Nat Commun*. 2022;13(1):1265.
42. Mirdita M, et al. ColabFold: making protein folding accessible to all. *Nat Methods*. 2022;19(6):679–82.
43. Yin R, et al. Benchmarking alphafold for protein complex modeling reveals accuracy determinants. *Protein Sci*. 2022;31(8):e4379.
44. Li X et al. Bioinformatic analysis of Roquin family reveals their potential role in immune system. *Int J Mol Sci*. 2024;25(11).
45. Schaefer JS, Klein JR. Roquin—a multifunctional regulator of immune homeostasis. *Genes Immun*. 2016;17(2):79–84.
46. Song J, et al. Human cytomegalovirus induces and exploits Roquin to counteract the IRF1-mediated antiviral state. *Proc Natl Acad Sci U S A*. 2019;116(37):18619–28.
47. Vogel KU, et al. Roquin paralogs 1 and 2 redundantly repress the Icos and Ox40 costimulator mRNAs and control follicular helper T cell differentiation. *Immunity*. 2013;38(4):655–68.
48. Pratama A, et al. Roquin-2 shares functions with its paralog Roquin-1 in the repression of mRNAs controlling T follicular helper cells and systemic inflammation. *Immunity*. 2013;38(4):669–80.

Publisher's note

Springer Nature remains neutral with regard to jurisdictional claims in published maps and institutional affiliations.